LA-UR-89-2246

COJR-8908120--2

LA-UR--89-2246

DE89 015241

TITLE: MOXE: AN X-RAY ALL-SKY MONITOR FOR THE SOVIET SPECTRUM-X-GAMMA MISSION

AUTHOR(S): W. C. Priedhorsky
E. E. Fenimore
C. E. Moss
R. L. Kelley
S. S. Holt

DISCLAIMER

Los Alamos
Los Alamos National Laboratory
Los Alamos, New Mexico 87545

MASTER

MOXE: an X-ray all-sky monitor for the Soviet Spectrum-X-Gamma mission

W. Priedhorsky, E. E. Fenimore, C. E. Moss
Earth and Space Sciences Division, Los Alamos National Laboratory

R. L. Kelley and S. S. Holt
Laboratory for High-Energy Astrophysics, Goddard Space Flight Center

ABSTRACT

We are developing a Monitoring X-Ray Experiment (MOXE) for the Soviet Spectrum-X-Gamma Mission. MOXE is an X-ray all-sky monitor based on array of pinhole cameras, to be provided via a collaboration between Goddard Space Flight Center and Los Alamos National Laboratory. Our objectives are 1) to alert other observers on Spectrum-X-Gamma and other platforms of interesting transient activity, and 2) to synoptically monitor the X-ray sky and study long-term changes in X-ray binaries. MOXE will be sensitive to sources as faint as 2 milliCrab (5σ) in 1 day, and cover the 2-20 keV band.

1. INTRODUCTION

X-ray stars include some of the most bizarre and fundamental objects in the Universe, like neutron stars and black holes. We have learned about these objects by studying their time variations, both rapid and slow. An all-sky X-ray monitor can measure variations in every bright X-ray star, with a resolution of seconds, over a baseline of years. The Soviet Spectrum-X-Gamma mission, scheduled for launch in 1993 and recently opened to US participation, offers an ideal platform for such a monitor.

Most x-ray instruments are pointed, and study one source at a time for no more than a few days. A monitor, which looks everywhere all the time, provides two capabilities: a real-time alarm for transient phenomena, and an archival record of changes in X-ray stars. The alarm capability allows more sophisticated instrumentation in X-ray and other bands to be alerted to transient events. For example, transient X-ray sources erupt several times per year in unexpected locations. If Spectrum-X-Gamma carries an X-ray monitor, its more sensitive narrow field-of-view instruments can be pointed at new transient sources to study them in detail. Observers at other wavelengths, including gamma-ray and ultraviolet astronomers with space-based instruments, and optical and radio astronomers working from the ground, can also study the transient before it fades away. Such studies have found our best candidates for black holes. The archive produced by a monitor allows long-term studies of changes in neutron star rotation rates, double star orbits, and accretion disk structure. We thus learn about the physics of mass transfer onto black holes and neutron stars.

Previous X-ray all-sky monitors have been insensitive, and none has operated since 1980. The present monitor on the Japanese Ginga satellite does not cover the whole sky and has a very low duty cycle. Eventually, an all-sky monitor on the Space Station should provide for the X-ray sky the same kind of data base provided to optical astronomers by the Harvard plates. Until then (1998?), there is a gap. The only all-sky monitor planned for the near-term is NASA's X-Ray Timing Explorer (1994?-1995).

We are developing a simple X-ray all-sky monitor for Spectrum-X-Gamma. The instrument will be a set of six X-ray pinhole cameras that stare continuously at the entire sky, with a bandpass of 2 to 20 keV. The detectors will be RC-readout position sensitive proportional counters. Data rates are low, and the instrument operates autonomously, with minimal interaction required between the instrument and rest of the spacecraft. A solid-state digital data recording system stores up to 32 hours of MOXE data.

Holt and Priedhorsky (1987) discussed the motivation for a pinhole-camera X-ray all-sky monitor, and a conceptual design. That paper led directly to the instrument now under construction. This paper represents that maturation of that design.

2. SCIENTIFIC OBJECTIVES

2.1 Historical perspective for an X-ray all-sky monitor

An X-ray all-sky monitor can provide two independent capabilities: a real-time alarm fc. transient phenomena, and an encyclopedic record for archival investigation. The extent to which a specific monitor can adequately provide these capabilities is a strong function of the detailed nature of the information sought. For example, a monitor designed only to signal the onset of strong solar flares does not require high sensitivity, storage capability or even location capability on the sky (since the flaring sun will unambiguously overwhelm the monitor response).

The extrasolar X-ray sky is dominated by the cosmic X-ray background (e.g. Marshall, et al. 1980) and the bright source Sco X-1, in the sense that a broad-band X-ray detector with omnidirectional response will have this "background" as the major contributor to its count-rate. The few-hundred brightest sources on the sky have both spatial and intensity distributions which suggest that they are largely confined to the plane of the Milky Way, while dimmer sources have both the spatial   otropic) and intensity $(N(>S) \sim S^{-3/2})$ distributions characteristic of a relatively uniform population of either intrinsically weak nearby sources or intrinsically strong extragalactic sources. Both types actually contribute, but the latter dominate as the number of dimmer sources exceeds the possible contribution from condensed sources in the galactic disk.

Marked temporal variability is almost ubiquitous on the X-ray sky. Only the gaseous nebulae of supernova remnants (<1% of the galactic source population) and galaxy clusters (perhaps 10% of the thousand brightest extragalactic sources, but a rapidly decreasing fraction of the dimmer source population) fail to exhibit detectable temporal variability. Truly periodic phenomena are generally associated with rotational or orbital periods, while aperiodic or quasiperiodic variability can have diverse origins. Shorter timescales generally describe smaller dimensional scales. Specific examples of variability will be discussed in the next section.

The alarm function of a monitor is its ability to signal anomalous variability, which can result in immediate follow-up investigation with other space-borne or ground-based instrumentation. Important unanticipated discoveries may result from the accidental detection of transient X-ray behavior. Early in the history of X-ray astronomy, for example, before sub-arc-second X-ray location capabilities existed, the "best" galactic black hole candidate Cyg X-1 was identified from simultaneous X-ray and radio flares (Tananbaum et al. 1972). More recently, the latest candidate for a black hole in the galaxy has been associated with the transient A0620-00 (which was the brightest X-ray source in the sky at its maximum) on the basis of prompt follow-up optical measurements (McClintock and Remillard 1986).

Whether or not X-ray variability detected by a monitor is used immediately to direct other instrumentation, the record of variability can be maintained for future archival study. This archival aspect of a permanent X-ray all-sky monitor should not be underestimated, in view of the empirical fact that temporal measurements have thus far provided the key to understanding some of the most important and basic aspects of X-ray sources, as reviewed briefly below.

2.2 All-Sky Monitor Astrophysics: Some Particular Examples

The long-term studies possible with an X-ray all-sky monitor will lead to new insight in the nature of accreting compact objects. Rather than be comprehensive, we discuss below some particular examples of the expected scientific yield from MOXE. Not included below are phenomena as important as long-term cycles in X-ray binaries, which have been reviewed by Priedhorsky and Holt (1987).

2.2.1 Luminous Low-Mass X-Ray Binaries
Thanks to quasi-periodic oscillations, interest in luminous low-mass X-ray binaries, like those in the Galactic bulge region, has been rekindled in recent years. Quasi periodic oscillations (QPO) are our first good handle on the near environment of the brightest X-ray stars in our Galaxy. Though these objects were the first X-ray stars discovered, we still understand them poorly. We presume them to be neutron stars, accreting matter from a low-mass companion and releasing radiant energy as the matter falls into the deep gravitational well of the neutron star. In 1985, two groups of investigators discovered quasi-periodic oscillations at 5-50 Hz in these objects (van der Klis et al. 1985; Middleditch and Priedhorsky 1986). Follow-up observations, especially by the EXOSAT satellite, showed similar oscillations in many luminous low-mass X-ray binaries. The oscillation phenomena may tell us about the spin rate and magnetic field of the neutron stars that are buried in the dense plasma environment of these systems.

Quasi-periodic oscillations exhibit a variety of behaviors that are strongly correlated with spectral state. Cygnus X-2 and other luminous low-mass sources trace out a regular "Z"-pattern in the hardness/intensity plane, with transitions that must correspond to changes in the geometry or stability of the accreting system. For example, the lower bend may correspond to a transition to super-Eddington accretion, with polar funnels and jets appearing in the accretion flow. Other low-mass X-ray binaries show non-"Z" patterns (Hasinger and van der Klis 1989).

MOXE would monitor the spectral-intensity variations of luminous binaries continuously. A bright bulge source of 500 milliCrab will yield 0.7 counts/s in the MOXE array, allowing an intensity measurement to 3% in a half hour. Since transitions along the spectral/intensity diagram take place with time scales of hours to days, MOXE will map the behavior of all bright bulge sources. We could learn how common the "Z-diagram" behavior is, what fraction of its time each source spends in each branch, and whether the Z and non-Z sources ever trade roles. As we better understand the spectral-intensity diagram, such observations will tell us the accretion rate behavior of the bulge sources, and whether there are instrinsic differences between sources (such as rotation rate or magnetic field). Detailed studies, such as QPO observations with larger Spectrum-X-Gamma instruments, will be facilitated by MOXE data. Observations can be carried out when the source is in the appropriate state. For example, the horizontal branch in Sco X-1 is very rare; QPO studies of this state can be triggered by MOXE spectral observations.

2.2.2 Accreting White Dwarfs

Cataclysmic variables (CVs) are semi-detached binary systems containing a white dwarf that is accreting material from a small companion star. They exhibit complex temporal and spectral behavior at X-ray wavelengths. CVs fall into two main classes: those with weak magnetic fields (chiefly the dwarf novae) and those with appreciable magnetic fields. The latter include those CVs showing large optical polarization in synchronism with the binary period (the "AM Her stars") and those showing coherent pulsations on a time scale of minutes (the "DQ Her stars"). The fields implied by these phenomena are between 10^6 and a few times 10^7 Gauss. In both types of system, magnetic fields channel the accretion flow onto one or more poles on the white dwarf. These stars therefore have complex optical and X-ray light curves which depend on the inclination of the binary system, the orientation of the accretion poles, and the amount of mass transferred from the companion star. They exhibit high and low X-ray states that occur on a time scale of months. The weakly magnetic dwarf novae have irregular intensity brightenings that occur every few weeks or months. These are marked by dramatic changes in the intensity level and spectrum which occur at all wavelengths. Many CVs have ultrasoft X-ray emission during optically bright states and almost all CVs observed reveal the presence of a variable "hard" component (2 - 10 keV) during all optical states. Several CVs will be bright enough to be detected with MOXE in a day. Interpretation of the origin of their X-ray emission and the nature of their variable temporal behavior depends on continuous, long-term monitoring. To date, these objects have been sampled only sporadically with pointing X-ray instruments. Observations with MOXE can answer a number of important questions regarding these objects, such as the nature of dwarf nova outbursts, and the geometry of accretion in magnetic cataclysmic variables.

2.2.3 Soft Gamma Repeaters: A New Class of Fast Transient

Soft Gamma Repeaters (SGRs) are a new class of objects (Laros et al. 1987; Atteia et al. 1987), very different from X-ray bursters and the classical gamma ray bursters (GRB), which are particularly appropriate for MOXE to monitor. Their typical photon energy is 30 keV whereas the X-ray bursters have typical energies 3 keV and the classical GRB have typical energies in excess of 300 keV. The classical GRB have very chaotic time histories lasting from less than a second to more than 1000 s, while the X-ray bursters have very simple time histories with a sharp rise and a decaying tail lasting tens of seconds. In contrast, the SGR have very sharp rises and falls with the whole event lasting the order of 0.1 s. There is no evidence that a classical GRB has ever repeated; minimum recurrence times are several years. The X-ray bursters have two different patterns of repetitions: Type I and Type II, corresponding to nuclear flash and accretion instability events. The SGR certainly do not have either of the those patterns (Laros et al. 1987). There is no correlation between event size and spacing; in fact, the third largest event of SGR1806-20 occurred within one second of the largest event and, yet, average size events can occur after almost any period of time. Only three SGRs are known: SGR1900+14, SGR1806-20, and SGR0526-22 (also known as the "March 5th" event; Mazets et al. 1982). These sources are extremely difficult to detect. There seems to be no pattern in how they recur and their short duration makes them appear as noise glitches in a detector. However, they are extremely bright, reaching 3000 Crab, so they can be easily detected in a 1 cm^2 detector. It was only good luck that one of the sources (SGR1806-20) was always within the narrow field of view of the UCB/Los Alamos X-ray and gamma-ray instruments on ISEE-3. SGR1806-20 was seen to repeat 110 times. The spectrum of SGR1806-20 falls sharply at low energy and is inconsistent with any self absorption or thermal process, but can be fit with a single Gaussian line at 18 keV, suggesting nearly pure cyclotron emission.

MOXE would have been able to detect all of these events as well as any comparable events from anywhere on the sky. Since MOXE is an imaging system, we can easily distinguish true events from noise glitches since a true event will occur only in a localized region of the detector. We have performed extensive Monte Carlo simulations of one year of MOXE data including orbital effects, the pinhole-detector geometry, the efficiency of the detector, the various backgrounds, and the presence of the Uhuru catalog sources. For a burst lasting 0.1 secs (the typical duration of a SGR), MOXE can detect events down to 2×10^{-6} erg/cm^2-sec. The brightest burst from SGB1806-20 was 7×10^{-5} erg/cm^2-sec and all 110 events were brighter than 2×10^{-6} erg/cm^2-sec. Spectrum-X-Gamma will thus be able to study in unprecedented detail a class of objects for which we know neither the galactic distribution, the mechanism of the energy release, nor the optical counterparts.

2.2.4. Gamma-Ray Bursts
The X-ray portion of the spectrum contains crucial information on the nature of classical gamma-ray bursts. A central mystery of gamma-ray bursts is why the bursts are gamma-ray events at all; that is, why the gamma-rays do not thermalize and produce many more X-rays than seen. Though X-rays are a small fraction of the total burst flux, gamma-ray bursts are still bright X-ray sources. X-ray data can tell if the spectrum becomes optically thick, whether there is an underlying X-ray source (necessary for some Comptonization models), and determine the continuum underlying cyclotron lines (Mazets et al., 1981). Ginga data showed a pair of spectral lines at 20 and 40 keV in one gamma burst, presumably from cyclotron absorption near a magnetic neutron star (Murakami et al. 1988; Fenimore et al. 1988). Confirming measurements would be valuable and require good measurements of the underlying continuum, especially in the region 10-20 keV. The continuum below the line is also important because that part of the spectrum cannot be easily produced by cyclotron processes. Based on a Monte Carlo simulation, we will be able to detect bursts down to a total fluence of 1×10^{-6} erg/cm^2, which translates into about 90 events per year. Of those, roughly 15 will have sufficient statistics (5 σ in more than half of the spectral bins) to do detailed spectral analysis. This is roughly 5 times as many as can be observed by the Los Alamos proportional counter/scintillator on Ginga.

2.2.5 X-Ray Transients
The value of an all-sky monitor like MOXE in alerting observers to transient X-ray sources is well-known. However, only recently have astronomers learned just how common moderate-luminosity transients are. The galactic plane survey by EXOSAT revealed several uncataloged bright X-ray sources (Warwick et al. 1985). Surveys by Ginga showed six uncataloged sources, 4 of which were not seen by the EXOSAT survey (Koyama 1988). The new sources had intensities from a few to a few tens of milliCrab, and include a large number of Be-neutron star binaries. Indeed, such transients may comprise the vast majority of galactic X-ray sources. MOXE has the sensitivity to track transients at this level. As a result, MOXE should track several transient sources at a time, and determine the frequency, luminosity function, and galactic distribution of moderate-luminosity transients.

2.2.6 MOXE and AGN Studies
There are two reasons to believe that the central energy sources in active galaxies contain black holes. These are the very large X-ray luminosities ($10^{41} - 10^{46}$ ergs/sec) and the rapid variations (down to ~ 1 hour or possibly shorter) in intensity, which indicate large masses ($>10^6$ M$_{sun}$) and compact size scales based on light-crossing time arguments. Prior to the launch of EXOSAT in 1983, there were only brief looks at active galaxies, using the Einstein Observatory and earlier instruments. These observations established that the flux from active galaxies (including QSO's) can be variable, but the timescales for variability was not well established, much less how the variability was related to other source properties (e.g., source luminosity). Observations with EXOSAT, with its long orbital period and large effective area over an extended bandpass, have shown that AGN are variable on timescales ranging from several hundred seconds to more than days. The Fourier power spectra of these sources typically show power law shapes (with slopes near unity) that extend over several orders of magnitude in frequency. Obviously, the power must roll over below some frequency and Pounds and McHardy (1988) suggest that on the basis of archival data the low-frequency "knee" is below 10^{-7} Hz. This is a tantalizing result worth following up. It hints that AGN are simply scaled-up versions of accreting stellar black holes like Cyg X-1. That ~10 M$_{solar}$ object shows a low-frequency knee at a few $\times 10^{-2}$ Hz (Nolan et al. 1981).

There are at least a dozen active galaxies for which MOXE will provide lightcurves with ~1 day time resolution. This timescale is interesting because it is there that power spectra are observed to roll over at low frequencies. Important sources include well-known bright active galaxies such as Cen A (which ranges from ~ 4 - 15 milliCrab) and NGC 4151 (2 milliCrab up to 12 milliCrab) and several BL Lac objects (Giommi et al. 1988; Schwartz and Madejski 1987). The fluxes of these objects are such that the Nyquist frequency will range from ~ 0.5 day to ~ 1

4

day, and the lowest measurable frequency should be below ~1 yr^{-1}. MOXE will thereby survey a new temporal regime for these objects

3. EXPERIMENTAL APPROACH: A TRADEOFF STUDY

MOXE is an X-ray all-sky monitor based on pinhole cameras. It has an all-sky field-of-view, ~3° angular resolution, ~millisecond temporal resolution, 2-12 keV (or greater) energy bandpass, and 2 milliCrab sensitivity in a 1-day exposure. In this section, we discuss the trade-off analysis which led to our experimental approach, which is a compromise between cost/complexity and scientific return.

X-ray all-sky monitors can be built with several approaches. To compare approaches, we compare scientific capabilities for a given level of resources (e.g. cost, power, telemetry). In the spirit of fairness, we therefore compare approaches that use the same values of gross detector area, detector positional resolution, overall field of view, and energy bandpass.

We are developing a baseline system of simple pinhole cameras for an X-ray all-sky monitor. It might at first appear that a system of scanning, slat-collimated proportional counters similar to the Ginga ASM could provide a simpler and cheaper alternative, since the counters need not be position-sensitive. The formal signal-to-noise ratio for each module of a comparable system (i.e. same gross detector area, field-of-view per resolution element, and overall field-of-view) is only a factor of two or so worse than for a pinhole system. The scanning system has comparable sensitivity because (to lowest order) its instantaneous area advantage is balanced by its decreased duty cycle. Each module is somewhat poorer than that of the baseline pinhole system because the scanning pinhole requires two crossed systems to determine source locations; even so, sources of similar brightness are ambiguously located.

Such a system of slat collimators has at least three other disadvantages relative to the baseline pinhole system. In attempting to normalize all approaches to the same resource requirements we have chosen a module field-of-view that is optimized for the baseline, but 1/6 of the sky is not the optimum module field-of-view for a scanning slat collimator system. Unlike the pinhole, which can cover the sky with six 1/6-sky modules (representing the six faces of a cube), scanning slats cannot do the same with six 1/6-sky great circle bands. In addition, a scanning system has a difficult time studying fast transient sources like the soft gamma repeaters. A more serious problem with this approach is that the need for a scan mechanism and an unobscured view of the sky present severe accommodation complications for a monitor not located on the outside of a spinning spacecraft (which Spectrum-X-Gamma is not). The need for moving parts rules out a scanning monitor for Spectrum-X-Gamma.

A more complex monitor might involve a group of reflecting telescopes arrayed to achieve full-sky coverage (for a fair comparison with the baseline, 1/6 of the system should be constrained to have a total detector area of 1000 cm^2). We reject such a system because the number of such telescopes would be very large, since grazing angles ~10 arc min are required for the desired energy range. In addition, monitors with focussing optics that have excellent sensitivity as formally evaluated, also have prohibitively large fabrication and/or accommodation costs. As such, they are not appropriate for a modest, low cost monitor system. This category includes a variety of options with reflecting surfaces, such as batteries of Wolter I telescopes offset from each other, "lobster eyes" (Angel 1979) or systems that might require optics that are conceptually straightforward but practically complex (e.g. Schmidt 1975).

Considering reliability and affordability for long-term unattended monitoring, the only true competitor to the simple pinhole is a coded aperture (i.e., a multiple-pinhole system based on URAs; Fenimore and Cannon 1978). As illustrated in Figure 1, this might appear to be a simple extrapolation of the single pinhole to larger area, but the signal extraction is qualitatively different. The multiple pinhole provides a multiplexing advantage of up to $N^{1/2}$, where N is the number of pinholes. However, there is a disadvantage to multiplexing because different sources contribute to the same detector element. As a result, the noise from every source contributes to the noise in each other, though there is no *systematic* crosstalk between sources. To compare these two systems and determine the sensitivity of the MOXE pinholes, we define the following parameters:
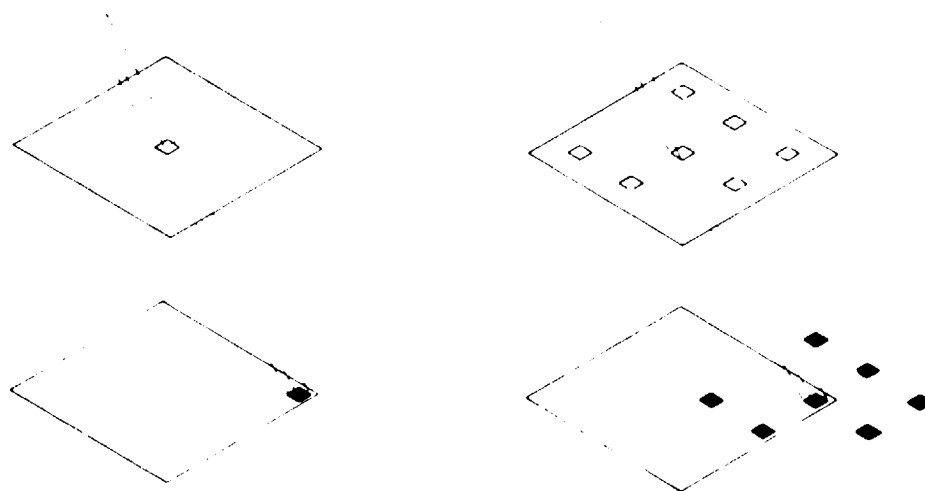
Figure 1. Simplified generalization of a single pinhole to a multiple pinhole. The multiple pinhole presents more active detector area to any direction on the sky. A source position is derived from the pattern of response across the entire detector surface.

S   = source intensity ($cm^{-2} \cdot s^{-1}$)
t   = total exposure time to source (s)
h   = duty cycle of exposure (fraction of unity)
e   = detector quantum efficiency from counter gas and window, including offset angle
A   = area of single pinhole (cm^2)
N   = number of pinholes per detector surface area
I   = internal detector background ($cm^{-2} \cdot s^{-1}$)
D   = diffuse background ($cm^{-2} \cdot s^{-1} \cdot sr^{-1}$)
f   = focal length = distance from mask to detector (cm).
Ω = solid angle subtended by a pinhole at distance f = A/f^2

Here we assume that the coded mask is 1/2 open and 1/2 closed, such that the total detector area is 2NA and the total field of view is $2N\Omega$ for the coded aperture.

The "signal" (total number of counts) measured from a source by a pinhole is given by:

$$Signal_{pin} = S(ht)Ae \qquad (1)$$

where the bracketed term represents the net time on t' source. The "signal" for the coded aperture is:

$$Signal_{ura} = S(ht)NAe. \qquad (2)$$

The "noise" relevant to the above signal is given by the square root of the total expected background plus the signal, upon which the signal rides:

$$Noise_{pin} = \{A(ht)(Se + I + \Omega De)\}^{1/2} \qquad (3)$$

and the URA "noise" is (Fenimore, 1978):

$$Noise_{ura} = \{A(ht)(NSe + 2NI + 2N^2\Omega De + Ne\Sigma S_i)\}^{1/2} \qquad (4)$$

6

where S_i are all the sources within the field of view.

Thus the pinhole signal-to-noise ratio is:

$$SNR_{pin} = Se \, [Se + I + \Omega De]^{-1/2} \, (Aht)^{1/2} \qquad (5)$$

and the coded aperture is:

$$SNR_{ura} = N^{1/2} Se \, [Se + 2I + 2N\Omega D + e\Sigma S_i]^{-1/2} \, (Aht)^{1/2}. \qquad (6)$$

If the diffuse background contributes most of the counts to a coded aperture, then the $2N\Omega D$ term dominates the noise and cancels the $N^{1/2}$ multiplexing advantage that derives from multiple pinholes. Indeed, for a MOXE-sized system and our limiting sensitivity of 2 milliCrab, the coded aperture offers no advantage.

However, the coded aperture SNR increases with source strength as S, while the pinhole increases only as $S^{1/2}$, so the coded aperture has a considerable advantage for brighter sources. For example, for a MOXE-sized system and a source of 50 milliCrab, the coded aperture gives twice the signal-to-noise of a pinhole. Thus the coded aperture is better for monitoring changes in bright sources, while the pinhole is better for detecting faint sources.

A separate question from source signal-to-noise is source detectability: the significance with which one can rule out the null hypothesis that there is no source. In that case, the noise term does not include the Se term, but only includes background statistics. For example, the significance of detection with a pinhole is:

$$Significance_{pin} = Se \, [I + \Omega De]^{-1/2} \, (Aht)^{1/2} \qquad (7)$$

Note that, for small numbers, equation (7) breaks down. One must detect a finite ($> \sim 5$) number of photons to have a detection.

Unfortunately, the coded aperture succeeds at the cost of a much higher count rate. The count rate for a pinhole is:

$$Rate_{pin} = A(e\Sigma S_i + 2IN + 2N\Omega De), \qquad (8)$$

while for the coded aperture the rate is:

$$Rate_{ura} = A(eN\Sigma S_i + 2IN + 2N^2\Omega De). \qquad (9)$$

The coded aperture count rate is higher by $\sim 2N^2\Omega D / \Sigma S_i$, which is a very large factor. Telemetering such a high count rate is beyond the capability of Spectrum-X-Gamma and, although we have developed several on-board processing techniques (Fenimore and Weston 1981, Fenimore 1987), these techniques require too much complexity in the data handling.

Better angular resolution could be achieved with linear detector resolution finer than the conservative one-part-in-64 adopted for MOXE system. However, even with state-of-the-art linear location capability of one part in 1000 (i.e. 10^6 resolution elements per detector), arc-second location capability would still be out of reach.

4. THE MOXE INSTRUMENT

4.1 The Baseline Approach for MOXE

We are developing an array of 6 X-ray pinhole cameras to provide all-sky monitoring on the Spectrum-X-Gamma observatory. This instrument will be called MOXE (Monitoring X-Ray Experiment). Figure 2 displays the MOXE system with the pinhole-to-detector distance f and the total active detector area chosen such that the field-of-view of the module is 1/6 of the sky (i.e. one face of a cube). In this case f is half the linear dimension of the detector; that is, $f \sim 1/2 \, [2NA]^{1/2}$. Actually, f is made slightly smaller such that there will be overlap between the modules even if there is a slight misalignment between them.
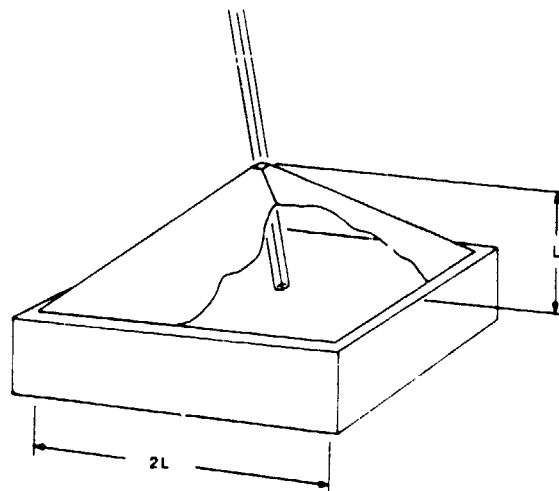
Figure 2. Conceptual design for a pinhole camera module with an overall field-of-view of approximately $2\pi/3$ steradians. A linear detector size that is twice the pinhole-to-detector distance defines the one-dimensional field-of-view to be ~90°. The pyramid-shaped mask has a single pinhole that allows a unique transformation between an area on the sky and a location on the detector surface.

The pinhole size should be made large enough such that I and ΩDe are comparable. Larger pinholes are "faster" in the sense that they reach the Poisson statistical limit for a given signal in a shorter time, but they offer no advantage in sensitivity if a short integration time is not critical, and they have poorer angular resolution. If $I = \Omega De$, then both terms contribute equally to the signal-to-noise; that requires $I = \Omega De = ADe/f^2 = 2De/N$, so that N is approximately $2De/I$. Thus, for modules that each view 1/6 of the sky, $I \sim \Omega De$ suggests a pinhole area that is about 1000 times smaller than the detector area (for the I and D below). For optimum resolution, each pinhole area should be oversampled by at least a factor of two in each dimension. As a matter of practicality, the state-of-the-art for imaging proportional counters can easily tolerate the ~64x64 resolution that would be required.

The final design consideration for our baseline system is the module size. Since the signal-to-noise is proportional to the exposure time and the area, the monitor "speed" scales as the square of its linear dimension. The mass of the system scales as its cube, so that for traditional cost models (which scale like the instrument mass to the 2/3 power), we are left with a linear relationship between monitor speed and cost. The numbers below follow from fixing the gross detector area at 1000 cm^2 and the pinhole area A at 1 cm^2:

$A = 1$ cm^2 $f = 16$ cm $\Omega = 4 \times 10^{-3}$ sr $h = e = 0.8$.

The backgrounds are:

$D = 3$ cm^{-2}s^{-1}sr^{-1} (3 - 6 keV)
$D = 8$ cm^{-2}s^{-1}sr^{-1} (2 - 12 keV)

$I = 3 \times 10^{-3}$ cm^{-2}s^{-1} (3 - 6 keV),
$I = 8 \times 10^{-3}$ cm^{-2}s^{-1} (2 - 12 keV),

1 Crab $= 1.4$ photons/cm^2 (3-6 keV)
$= 1.0$ my (5.5 keV) $= 947$ UFU
$= 2.4 \times 10^{-8}$ erg-cm^{-2}-s^{-1} (2-10 keV).

The parameter h anticipates exposure-reducing factors for typical viewing conditions, and I represents twice the minimum background experienced in orbit with similar detectors (e.g., on HEAO-1). Backgrounds in the 3-6 keV band are used to estimate sensitivities (conservatively), and those in the 2-12 keV band are used to estimate detector count rates.

4.2   Experimental Capabilities

The detection limit of the MOXE system is shown in Figure 3. The detection limit corresponds to a 5-sigma significance of detection in the 3-6 keV band (equation 7). In a 1-day exposure, MOXE can detect sources down to 2 milliCrab (5σ); in 1 hour, 9 milliCrab; in 1 minute, 72 milliCrab; and in 1 second, 4.5 Crab. For short exposures (< 60 s), the detection limit of Figure 3 requires 5 source counts, because the background is less than 1 count. True galactic "transients" (i.e. hard X-ray emission with peak luminosity > 10^{36} erg/s and decay time > 1 day) should be detectable anywhere in the galaxy, and factor-of-two variability can be observed in ~100 galactic sources on timescales of an hour or more.
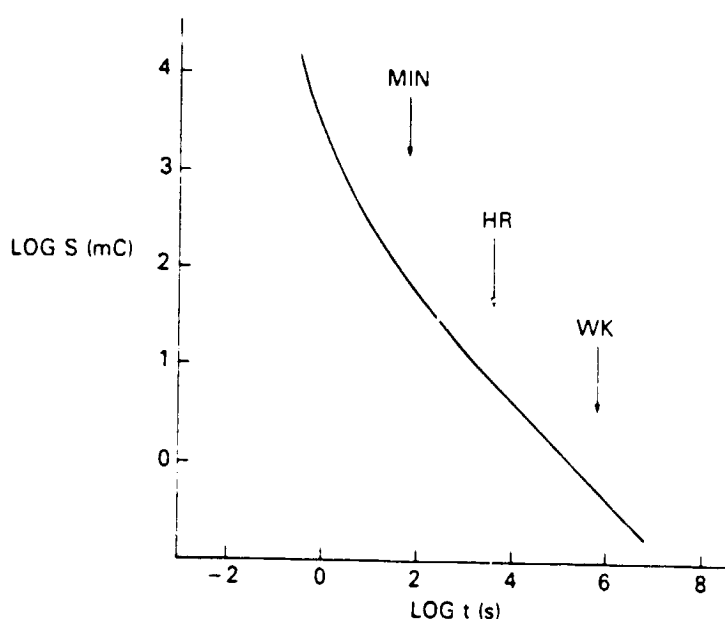

Figure 3. Five-sigma detection limit of the MOXE pinhole camera system (equation 7), with the average exposure efficiency parameters discussed in the text, as a function of gross accumulation time. The trace diverges from the analytic (straight-line) relation by requiring 5 recorded source counts when the expectation value of the total background is less than 1 count. The arrows signal the detection limit for 1 min, 1 hr, and 1 week.

Our positional point-spread function (PSF) is estimated from the various blurrings that can contribute. The FWHM of the PSF is roughly one-half of the effective pinhole size divided by the focal length. The effective pinhole size can be found from the convolution of the true pinhole size (1.0 cm), the readout pixel size (0.5 cm), and the PSF of the detector (~0.5 cm). Estimating the convolution by adding these values in quadrature gives a PSF of $\tan^{-1}$ [(3)$^{1/2}$/ 2/ 16] or 2.2 degrees. Centroiding can give position to about one-tenth of that or 15 arc minutes.

Since each 1/6-sky module will have ~4 strong (> 100 milliCrab) sources in its total field-of-view on the average, and each of these sources will contribute ~ 10^4 counts per day, the strong source network is capable of defining aspect for each modules *independently* to an absolute accuracy of the order of 15 arc minutes. Considering a monitor fixed in inertial space, for example, and the worst case situation where the source centroid is close to the corners of four detector elements, the daily accumulation in each of the four strong-source elements will be > 3/16x2000=375 above an average background of ~300. This estimate is conservative, because some of the bright sources will be stronger than 100 milliCrab. Any uncertainty (or variability) in source magnitude is immaterial. Note that similar centroid determination is possible even when the monitor drifts in celestial coordinates, provided

9

that the angular drift between readouts is less than the angular resolution of the monitor; if not, the effective background will be larger, since the image will be spread among more pixels per readout.

Bright (> 100 milliCrab) transients can be located to < 15 arc min with the baseline system, but ~1 day would be required to achieve such precision. If we can take advantage of independent information, such as spacecraft aspect data, the determination can be made even faster since the largest uncertainty will be the (good) counting statistics of the transient, itself. Under these circumstances a transient as bright as A0620-00, for example, which reached a maximum intensity of ~50 Crab, can then be located to < 15 arc min in ~2 temporal minutes. In any case, the location of 100 milliCrab transients to < 60 arc min can always be accomplished on timescales < 1 hour (~100 counts allows the source to stand out clearly from the background, but the statistics for centroiding are limited). The total count contribution from a 10 milliCrab transient is comparable to the total background in one pixel, so that location to ~1 degree will require an accumulation time ~1 day.

The baseline system of 6 modules is capable of monitoring the whole sky on timescales > 1 week for sources as faint as ~1 milliCrab ~ 1 UFU that are separated by a few degrees with no source confusion. Every 10 milliCrab source can be monitored on timescales of an hour, and bright (> 100 milliCrab) sources can be monitored on timescales of minutes. Only the brightest dozen sources can be monitored with the baseline system on timescales less than one minute; we shall, therefore, adopt one minute as the baseline minimum readout time, with ~msec time resolution much preferred.

Since the total expected counting rate from the six modules is ~100 counts s^{-1} (with less than half from monitorable sources), each detected photon can be encoded in 32 bits (one of 4096 elements in each of the 6 modules and 16 energy channels, with 12 time bits) at a telemetry rate of 3.2 kbps, with no losses on the average. Bright spots on the sky (the Sun and Sco X-1) can be masked out of the telemetry stream to reduce telemetry. For the MOXE experiment on Spectrum-X-Gamma, we require 50% extra telemetry (5.0 kbps) to allow for very bright transients, unexpected background count rates, and special readout of triggered burst events. High on-orbit count rates can also be accommodated by electronically narrowing the telemetry window to somewhat less than 2-20 keV.

Intense flux from the Sun, the brightest source in the X-ray sky, raises a particular problem. Since MOXE covers 4π steradians, the Sun will always be in view of at least one detector. During times of quiet Sun, the Sun is simply a telemetry problem. These events must be masked so as not to saturate our data stream with uninteresting solar data. During solar maximum, the Sun can be so intense as to damage the detector, with 10^5-10^6 photons/cm^2/sec typical outside of flares (1-8 Å), and up to 100 times more at flare maximum. At such times, the detector high voltage must automatically switch off to protect the detector.

The accommodation of single pinhole modules on the Spectrum-X-Gamma platform is particularly straightforward. Only the 1 cm^2 pinhole at the end of the tapered pyramidal collimator need be unobscured. The six modules can be arranged to each have slightly > 1/6-sky coverage, so that the "seams" are still covered if the cube faces are slightly misaligned. The six modules are independent (except for shared low voltage power supplies), have modest resource and accommodation requirements, are based on proven, inexpensive technology, and have no inherent lifetime limitations. The pointing directions of any and all are not critical and do not require external verification.
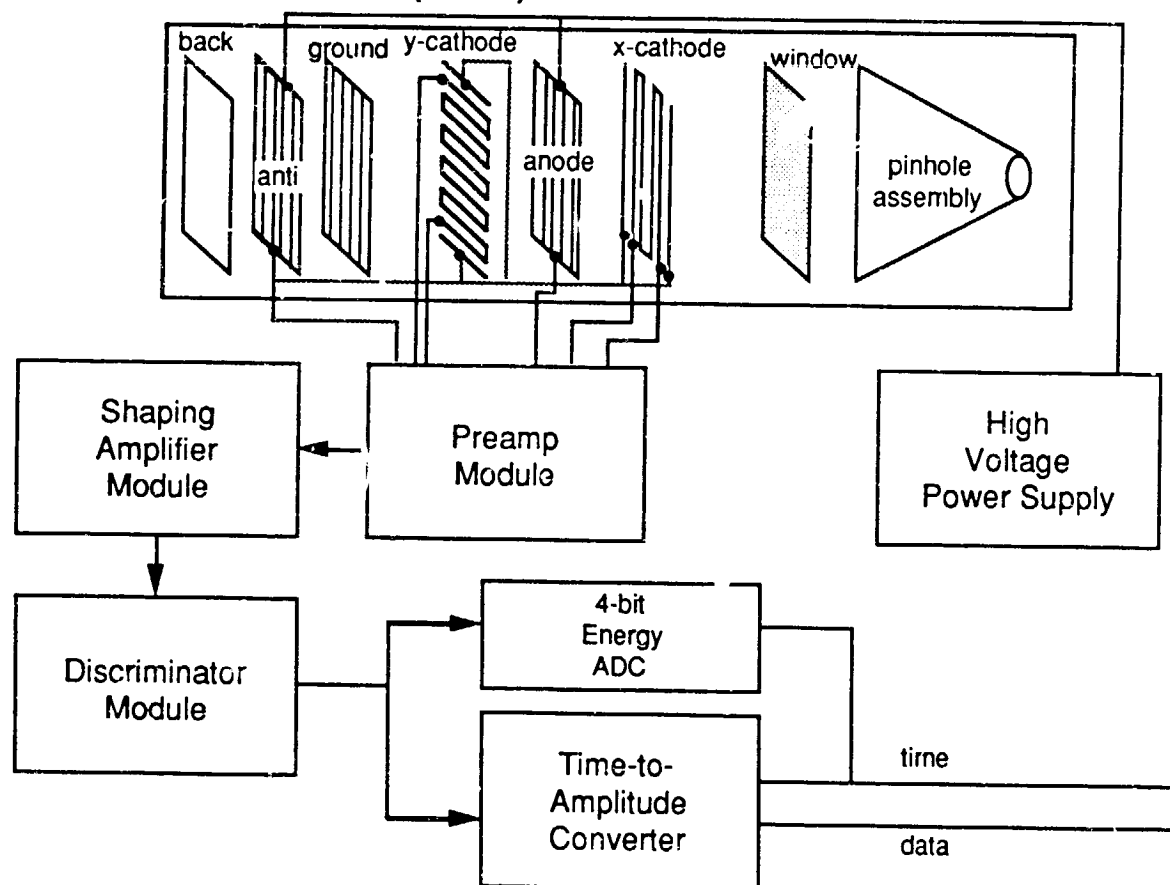
4.3 Hardware Realization of MOXE

MOXE consists of an array of 6 X-ray pinhole cameras, and associated digital and analog electronics. Each pinhole camera unit weighs 15 kg, has a volume of about 45 x 45 x 32 cm, uses 5 Watts, and requires ~800 bits per second. The central electronics module weighs 29 kg and draws 23 Watts of conditioned power. The pinhole cameras will include detectors, high voltage power supplies, and preamplifiers. Each camera will interface to the central electronics module for A/D conversion, event analysis, commanding, telemetry, data memory, interface to the satellite, and low voltage power supply. The system block diagram is shown in Figure 4. Because Spectrum-X-Gamma flies outside the Earth's magnetosphere, it encounters a high radiation dose. All electronics will be designed to withstand at least 10^4 rads.

4.3.1 Detectors
The active sensors for MOXE are position-sensitive proportional counters. The resolution requirement for MOXE (64 x 64 elements) is very modest; we can meet this requirement by using proven, commercially available detector technology. We will use sealed proportional counters with RC position encoding (Borkowski and Kopp 1972).

Channel Module (1 of 6)
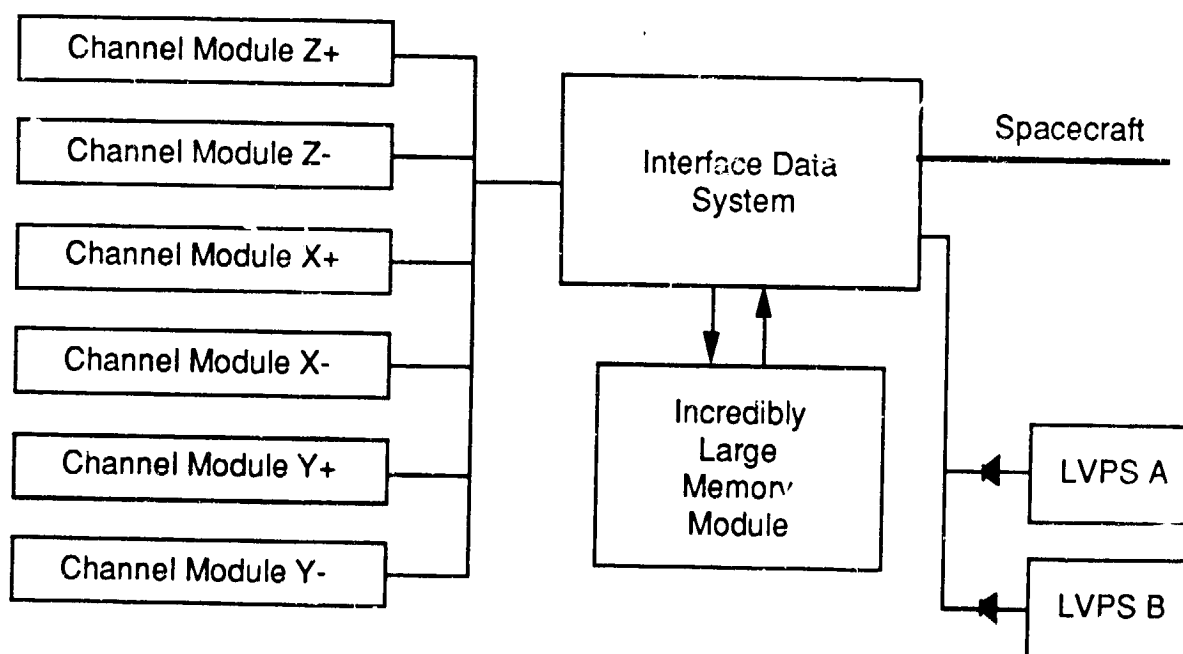

System Interconnection

Figure 4. Block diagram of the MOXE experiment.

Position signals will be read out from two orthogonal "meanders" of high resistance wire (the x and y cathodes). The rise time of the four signals (one from each end of each wire) will be proportional to the position of the photon interaction. Each detector's active area will be 32 x 32 cm, and it will be filled with Xe-CO_2 counting gas at atmospheric pressure or slightly above. Similar sealed detectors built by the Goddard group have remained stable for more than 10 years. The expected position resolution, 0.5 cm, will be sufficient for our requirements. 5-sided anti-coincidence and pulse shape discrimination will be used to reject cosmic ray background. An anti-coincidence plane will cover the full area of the detector below the main detector volume, while the ends of the x- and y-cathode arrays will provide anticoincidence volumes to guard the sides. All 5 anti-coincidence wires will be fed into a single preamp to yield a guard signal. Energy resolution will be standard for a proportional counter, 20% or better (FWHM) at 6 keV.

The low-energy cutoff will be set by the entrance window, which will be selected based on its transmission of cosmic X-rays, absorption of low-energy Solar flux, and ease of integration. Candidate windows range from 0.001" Mylar to 0.005" beryllium. A pyramidal assembly will hold the 1 cm^2 pinhole ~16 cm above the detector (as in Figure 2). The window support assembly must have minimal obscuration, even for rays striking the detector at angles greater than 45°, but must support the window against a load of about 2000 kg. Alternately, we may fill the pyramid volume with helium at almost same pressure as the detector. This would minimize the differential across the large window and allow a more modest support structure.

4.3.2 Analog Electronics
The high voltage power supplies (HVPS) will produce a nominal +2700 VDC. This level will be commandable to adjust the detector gain. There will be one HVPS per detector. The preamplifier will be "voltage sensitive". The preamplifiers will preserve the proportionality of the rise time to interaction position and provide sufficient gain to preserve the signal to noise ratio from the detector. A single additional preamplifier will process pulses from five interconnected anticoincidence electrodes.

The shaping amplifier will consist of a set of amplifiers which will produce the time derivative of the input (pre-amp) signal. This will produce a output signal which will have a zero-crossing at the time the input signals peak. This module will also sum the outputs of the four signals from the detector/preamp system and produce two signals necessary for further processing: 1) The sum signal, which is proportional to the total energy of the incident photon will be sent to the "Energy Analyzer Module" and resolved in one of 16 energy levels. 2) A parallel sum signal, which will be sent to a differentiator which will produce a signal which will cross zero at a known and constant time after the interaction of the photon in the detector. This signal will be used to strobe the time into readout memory.

The discriminator module (DSM) will detect the zero crossings of the individual x and y detector output signals as well as that of the sum signal. This will produce signals to start and stop the time-to-amplitude converter and start the energy ADC. The DSM will also perform a level discrimination on the "anti" signal and produce a flag if that signal exceeds a commandable level. A time-to-amplitude converter will produce a 12-bit digital word which is proportional to the x and y positions of the photon interaction in the detector. An energy ADC will produce a four-bit digital word which will resolve the sum signal into one of 16 energy bins using a low power sample-and-hold analog-to-digital converter system.

4.3.3 Digital Electronics
There will be one interface data system (IDS) to service the six channel modules of the MOXE instrument. The heart of the IDS will be an 80C86RH micro processor which will respond to interrupts from the channel modules. On receiving a request for service the IDS will command the module on the data bus where it will be read and placed in memory for future readout. The data will consist of 32 bits: 12-Photon Position, 4-Photon Energy, 3-Detector ID, 12-Time, and 1 for the Anti-coincidence flag. The IDS will also receive the commands from the spacecraft environment, check them for validity, and pass them on to the appropriate sub-unit on a command bus.

Instruments on Spectrum-X-Gamma are required to store data for up to 32 hours between transmissions to the ground. For MOXE, the time-averaged 5.00 kbps rate requires storage of 576 Mbits, plus error detection and correction bits. We will build this memory from 256K SRAM technology, in a simple FIFO design controlled by an 80C86RH microprocessor chip. The memory unit is called the ILMM (Incredibly Large Memory Module). Single bit upsets are handled by error detection and correction software which continuously cycles through the memory when the processor is not otherwise tasked.

5. CONCLUSION

Most of our knowledge of X-ray sources comes from their time variability, as glimpsed in occasional observations by small field-of-view instruments. Such true monitoring over a large portion of the sky has been accomplished only by the Vela and Ariel-5 satellites (see Priedhorsky and Holt, 1987, for a review of the instrumentation which has been used for monitoring the X-ray sky). At present, there is no such monitor capability in orbit. The Japanese Astro-C (Makino et al. 1986), launched in February 1987, provides partial sky coverage with a low duty cycle, and will probably not work into the Spectrum-X-Gamma epoch. MOXE will monitor the sky in an epoch otherwise uncovered, observing all bright X-ray sources all of the time.

6. ACKNOWLEDGEMENTS

7. REFERENCES

Angel, J. R. P.: 1979, *Astrophys. J.* 223, 364.
Atteia, J.-L. et al.: *Astrophys. J. (Letters)* 320, L105.
Borkowski, C. J., and Kopp, M. K.: 1972, *IEEE Trans. Nucl. Sci.* NS-19 (3), 161.
Fenimore, E. E.: 1978, *Appl. Opt.* 17, 3562.
Fenimore, E. E.: 1987, *Appl. Opt.* 26, 2760.
Fenimore, E. E., and Cannon, T. M.: 1978, *Appl. Opt.* 17, 337.
Fenimore, E. E., and Weston, G. S.: 1981, *Appl. Opt.* 20, 3058.
Fenimore, E. E. et al.: 1988, *Astrophys. J. (Letters)* 335, L71.
Giommi P., et al.: in *Physics of Accretion onto Compact Objects: Theory vs. Observations.* COSPAR-IAU symposium, Sofia, Bulgaria.
Hasinger, G., and van der Klis, M.: 1989, *Astron. Astrophys.*, in press.
Holt, S. S., and Priedhorsky, W.: 1987, *Space Sci. Rev.*, 45, 269.
Koyama, K.: 1988, preprint.
Laros, J. G. et al.: 1987, *Astrophys. J. (Letters)* 320, L111.
Makino, F., et al.: 1986, *The X-Ray Astronomy Satellite Astro-C*, ISAS Research Note #326, Institute of Space and Astronautical Science, Tokyo.
Marshall, F. E., Boldt, E. A., Holt, S. S., Miller, R. B., Mushotzky, R. F., Rose, L. A., Rothschild, R. E., and Serlemitsos, P. J.: 1980, *Astrophys. J.* 235, 4.
Mazets, E. et al.: 1981, *Nature* 290, 378.
Mazets, E. et al.: 1982, *Astrophys. Space Sci.* 80, 173.
McClintock, J. E. and Remillard, R. A.: 1986, *Astrophys. J.* 308, 110.
Middleditch, J., and Priedhorsky, W.: *Astrophys. J.* 306, 230.
Murakami, T. et al.: 1988, *Nature* 335, 234.
Nolan, P. L. et al.: 1981, *Astrophys. J.* 246, 494.
Pounds, K. A., and McHardy, I. M.: 1988, in *Proceedings of the Conference on Neutron Stars and Black Holes*, ed. Y. Tanaka. Tokyo.
Priedhorsky, W. and Holt, S. S.: 1987, *Space Sci. Rev.*, 45, 291.
Schmidt, W. H. K.: 1975, *Nucl. Instr. Meth.* 127, 285.
Schwartz, D. A., and Madejski, G. M.: 1987, in *Proceedings of the Conference on Variability of Galactic and Extragalactic X-Ray Sources.* Como, Italy.
Tananbaum, H., Gursky, H., Kellogg, E., Giacconi, R., and Jones, C.: 1972 *Astrophys. J.* 177, L5.
van der Klis, M., Jansen, F., van Paradijs, J., Lewin, W. H. G., van den Heuvel, E. P. J., Trümper, J., and Sztajno, M.: 1985, *Nature* 316, 225.
Warwick, R. S., Turner, M. J. L., Watson, M. G., and Willingale, R.: 1985, *Nature* 317, 218.